

Clinic Correlation and Prognostic Value of P4HB and GRP78 Expression in Gastric Cancer

Zhang C¹, Zhao W², Zhang X³, Zhang X¹, Song L¹, Xu W¹, Chen X³ and Yang L^{1*}

¹Department of Medical Oncology, Affiliated Tumor Hospital of Nantong University, 30 Tongyang North Road, Nantong 226361, China

²Department of Cancer Research, Affiliated Tumor Hospital of Nantong University, 30 Tongyang North Road, Nantong 226361, China

³Department of Pathology, Affiliated Tumor Hospital of Nantong University, 30 Tongyang North Road, Nantong 226361, China

*Corresponding author:

Professor Lei Yang,
Department of Medical Oncology, Affiliated
Tumor Hospital of Nantong University, 30
Tongyang North Road, Nantong 226361, China,
E-mail: 591623249@qq.com

Received: 23 Feb 2022

Accepted: 04 Mar 2022

Published: 11 Mar 2022

J Short Name: COO

Copyright:

©2022 Yang L. This is an open access article distributed under the terms of the Creative Commons Attribution License, which permits unrestricted use, distribution, and build upon your work non-commercially.

Citation:

Yang L, Clinic Correlation and Prognostic Value of P4HB and GRP78 Expression in Gastric Cancer.

Clin Onco. 2022; 6(3): 1-14

Keywords:

Gastric cancer; P4HB; GRP78; Risk factor; Nomogram

1. Abstract

1.1. Background: Prolyl 4-hydroxylase, beta polypeptide (P4HB) and Glucose-regulated protein 78 (GRP78) represent for poor prognosis of various cancers, while rare research investigate correlation of them. This study aimed to explore correlation and prognostic value of them in gastric cancer (GC).

1.2. Methods: 150 GC tissue samples evaluated P4HB and GRP78 protein expression by immunohistochemistry separately, the association of them with clinicopathological features was analyzed. To explore correlation between their mRNAs and pathways, bioinformatics analyses were performed. Kaplan-Meier analyses were taken to compare survival curves. Univariate and multivariate Cox regression models were used to find potential prognostic factors of overall survival (OS). Then a prognostic nomogram was constructed, whose discrimination ability and clinical usefulness were compared to TNM stage

1.3. Results: P4HB protein positive correlated with GRP78, as the same tendency of mRNAs in databases. Bioinformatics analyses indicated P4HB and GRP78 may be associated with protein folding and response to ER stress, and with the protein processing in ER pathway. High single expression or co-expression of P4HB and GRP78 indicated a shorter OS. When stratified by postoperative adjuvant chemotherapy, high co-expression was only represented for unfavorable prognosis in the group with chemotherapy, especially in advanced stage. Multivariate Cox regression analysis identified differentiation ($P = 0.020$), TNM stage ($P < 0.001$), postoperative adjuvant chemotherapy ($P = 0.005$) and P4HB and clinicsofoncology.com

GRP78 co-expression ($P = 0.002$) were independent prognostic factors for OS. The nomogram was better than TNM stage in discrimination ability and clinical usefulness from receiver operating characteristic (ROC) and decision curve analysis (DCA) curves.

1.4. Conclusion: P4HB may positive correlate with GRP78 expression in GC. Co-expression of them can be an independent prognostic factor, serving as a predictive biomarker for GC patients, especially for advanced stage with postoperative adjuvant chemotherapy. The nomogram may be better than TNM stage in discrimination ability and clinical usefulness.

2. Introduction

Gastric cancer (GC) is the fifth common diagnosed cancer and the third frequently cause of cancer death global wide, relating to over one million new cases and an estimated nearly zero point eight million deaths in 2018, while the incidence rate is still notably elevating in Eastern Asia [1]. Since the best treatment period of most GC patients had already missed when they clinically diagnosed, the prognosis of GC remains poor [2]. The grim fact that survival trends were little increased in most countries between 1995–1999 and 2010–2014 disappoints us, and the efforts to improve treatment strategies seem in vain [3]. Owing to huge biological heterogeneity, even with similar clinical features, the prognoses of GC would perform great differences [4, 5]. Therefore, precisely evaluate the prognosis of GC with the aid of better predictors is urgently needed. The endoplasmic reticulum (ER) is responsible for lipid biogenesis, calcium dynamic balance, and participate in folding proteins. Once various stresses such as hypoxia destroy

the homeostasis, the resulting abnormal accumulation of unfolded and misfolded proteins together constitute ER stress [6]. A series of signaling pathways named unfolded protein response (UPR) subsequently activates to reconstruction ER homeostasis, which involve three main branches: 1) PERK (pancreatic ER kinase-like ER kinase, also known as eIF2AK3)–eIF2 α (eukaryotic translation initiation factor 2 α); 2) ATF6 (activating transcription factor-6); 3) IRE1 (inositol-requiring protein 1, also known as ERN1)–XBP1 (X-box binding protein 1) [6-8]. Tumors tend to accompany with hypoxia, acidosis and nutrient deprivation, frequently induce ER stress, together with follow-up activation of UPR, play core roles in tumorigenesis, proliferation and survival of cancer cells [6].

Prolyl 4-hydroxylase, beta polypeptide (P4HB, also known as PDIA1) belongs to protein disulfide isomerase (PDI) family, as an enzymatic molecular chaperone to reconstruct misfolded proteins, close connects with ER stress and UPR [9]. P4HB is proved to be upregulated in a variety of cancers, such as diffuse glioma [9], lung cancer [10], and colon cancer [11]. As a result, P4HB has been reported by numerous researches to be a potential target for cancer therapy [12-14]. But studies involved GC were rather limited. Only one recent research showed P4HB positive correlated with hypoxia-associated biomarkers, overexpression of P4HB indicated poor prognosis in GC patients [15].

Glucose-regulated protein 78 (GRP78, also known as HSPA5 or BiP) also acts as an ER chaperone protein, dissociates from three specific sensors (PERK, ATF6 and IRE1) in response to ER stress, activates UPR subsequently [16]. General overexpression of GRP78 in different cancers including GC has been widely accepted, and GRP78 could also serve as a good indicator of poor prognosis and contribute a lot to therapy resistance [17, 18]. Xia et al identified that P4HB through downregulating GRP78 promoted hepatocellular cancer tumorigenesis [19]. In GC, single overexpression of the two ER chaperone proteins has been reported to represent

poor prognosis, indicating P4HB may not negative correlate with GRP78. Due to rare relevant research, we aimed to investigate the correlation between P4HB and GRP78 expression and clinical features, as well as their prognostic values in GC. Furthermore, we integrated the expression of P4HB and GRP78 with other prognostic variables to predict overall survival (OS) after surgery of GC patients.

3. Materials and Methods

3.1. Patients

In our retrospective study, amount to 150 GC patients who underwent gastrectomy from 2007 to 2013 at Affiliated Tumor Hospital of Nantong University (Nantong, China) were enrolled. The median follow-up time was 68.0 (range 2.5 -92.5) months. All patients confirmed histopathology diagnosis after gastrectomy, none of whom received preoperative radiotherapy or chemotherapy. Patients histopathological diagnosed adenosquamous or neuroendocrine carcinoma, as well as with incomplete follow-up data were excluded from the cohort. The clinicopathological parameters included were shown below: age, gender, Bormann type, tumor size, Lauren's classification, differentiation, histological type, depth of tumor invasion, lymph node metastasis, tumor-node-metastasis (TNM) stage, vessel invasion, perineural invasion and fluorouracil-based postoperative adjuvant chemotherapy (sTable 1 and sTable2). The TNM stage referred to 7th edition of TNM Staging Manual from the American Joint Committee on Cancer (AJCC), and fluorouracil-based postoperative adjuvant chemotherapy were mainly performed in advanced TNM stage patients. Overall survival (OS) was defined as the period between the date of gastrectomy with the date of death or last follow-up. Data were censored, if patients ended follow-up in keeping alive. The study had achieved the approval from the informed consent of all patients and the Ethics Committee of Affiliated Tumor Hospital of Nantong University.

sTable 1: Clinicopathological characteristics of GC patients

Clinicopathological parameters	n	%	Clinicopathological parameters	n	%
Age(year)					
<65	83	55.3	≥65	67	44.7
Gender					
Male	103	68.7	Female	47	31.3
Bormann type					
I / II	52	34.7	III / IV	98	65.3
Tumor size(cm)					
<5	83	55.3	≥5	67	44.7
Lauren's classification					
Intestinal	31	20.7	Diffuse	71	47.3
Mixed	48	32			
Differentiation					

Well/Moderate	60	40	Poor	90	60
Histological type					
Adenocarcinoma	139	92.7	Mucinous/Signet-ring cell	11	7.3
Depth of tumor invasion					
T1/T2/T3	104	69.3	T4	46	30.7
Lymph node metastasis					
Negative	51	34	Positive	99	66
TNM stage					
I / II	72	48	III / IV	78	52
Vessel invasion					
Negative	106	70.7	Positive	44	29.3
Perineural invasion					
Negative	115	76.7	Positive	35	23.3
Postoperative adjuvant chemotherapy					
No	50	33.3	Yes	100	66.7

sTable 2: Correlation between P4HB and GRP78 protein expression in different clinicopathological characteristics of GC patients

Clinicopathological parameters	Correlation coefficients	P value	Comparison of correlation coefficients	
			Z	P value
Age(year)				
≥65 vs. <65	0.576 vs. 0.571	<0.001 vs. <0.001	0.044	0.965
Gender				
Female vs. Male	0.661 vs. 0.569	<0.001 vs. <0.001	0.821	0.412
Bormann type				
III / IV vs. I / II	0.581 vs. 0.636	<0.001 vs. <0.001	-0.497	0.619
Tumor size(cm)				
≥5 vs. <5	0.703 vs. 0.480	<0.001 vs. <0.001	2.088	0.037
Lauren's classification				
Diffuse vs. Intestinal	0.627 vs. 0.559	<0.001 vs. 0.001	0.468	0.64
Mixed vs. Diffuse	0.589 vs. 0.627	<0.001 vs. <0.001	-0.314	0.754
Mixed vs. Intestinal	0.589 vs. 0.559	<0.001 vs. 0.001	0.186	0.853
Differentiation				
Poor vs. Well/Moderate	0.655 vs. 0.483	<0.001 vs. <0.001	1.509	0.131
Histological type				
Mucinous/Signet-ring cell	0.661 vs. 0.561	0.027 vs. <0.001	0.441	0.66
Vs. Adenocarcinoma				
Depth of tumor invasion				
T4 vs. T1/T2/T3	0.662 vs. 0.568	<0.001 vs. <0.001	0.834	0.405
Lymph node metastasis				
Positive vs. Negative	0.615 vs. 0.517	<0.001 vs. <0.001	0.819	0.413
TNM stage				
III / IV vs. I / II	0.713 vs. 0.457	<0.001 vs. <0.001	2.396	0.017
Vessel invasion				
Positive vs. Negative	0.740 vs. 0.528	<0.001 vs. <0.001	1.966	0.049
Perineural invasion				
Positive vs. Negative	0.432 vs. 0.625	0.010 vs. <0.001	-1.351	0.177
Postoperative adjuvant chemotherapy				
Yes vs. No	0.630 vs. 0.598	<0.001 vs. <0.001	-0.289	0.773

3.2. Immunohistochemistry (IHC)

The tissue microarrays (TMA) were constructed by duplicate 1.5 mm formalin-fixed paraffin-embedded tissue cores of two different areas. IHC was performed according to the standard protocol for the immunostaining provided by a previous study [20]. P4HB expression used a mouse anti-P4HB monoclonal antibody (1:100, Abcam, Cambridge, UK), while GRP78 IHC used a rabbit anti-GRP78 monoclonal antibody (1:100, Abcam, Cambridge, UK). The mi-quantitative H-score, ranged from 0 to 300, was derived from the staining intensities (0, 1, 2, 3 respective stand for negative, weak, moderate, strong staining) and the proportion of stained (0–100%). Two experienced pathologists who were blind to clinical information evaluated H-scores independently. The P4HB and GRP78 median H-scores as cutoff values were both 200, H-scores less than 200 were considered to low expression, otherwise were considered to high expression.

3.3. Bioinformatics analyses

The interactive web server GEPIA (<http://gepia.cancer-pku.cn/index.html>) [21], based on The Cancer Genome Atlas (TCGA), was used to find the correlation of mRNAs in GC tissue. And the mRNA expression data of 37 GC cell lines was downloaded from CCLE (<https://portals.broadinstitute.org/ccle>) [22]. Gene Ontology (GO) and Kyoto Encyclopedia of Genes and Genomes (KEGG) analysis were carried out by R package “clusterProfiler”. Besides, R package “pathview” was performed to visualize the correlation coefficients of genes in KEGG pathway maps.

3.4. Statistical analysis

SPSS version 25.0 (IBM, Armonk, NY) was applied to for the χ^2 test to explore the correlations among biomarker variables and clinicopathological variables, the Spearman rank correlation to evaluate the relationship, the univariate and multivariate anal-

yses by the stepwise Cox proportional hazard regression model to estimate the hazard ratios (HRs) and 95% CI of HRs. MedCalc Software version 19.0.4 (MedCalc, Mariakerke, Belgium) was applied to compare two correlation coefficients. The R packages “rms”, “survival”, “foreign”, “survivalROC” and “survminer” were used for plotting nomogram, calibration curves, receiver operating characteristic (ROC) curves and Kaplan–Meier curves. Decision curve analysis (DCA) curves were plotted by R package “stdca”, whose source file was from www.mskcc.org. Two-sided P value less than 0.05 was considered statistically significant.

4. Results

4.1. Association of P4HB and GRP78 protein expression with clinicopathological characteristics in GC

We detected the expression of P4HB and GRP78 protein separately by IHC in 150 GC tissues. The representative images of P4HB and GRP78 staining are shown in (Figure 1). 74 patients (49.3%) low expressed P4HB and 76 patients (50.7%) high expressed P4HB, as for GRP78, there were 71 low cases (47.3%) and 79 high cases (52.7%) respectively. Furthermore, the expression of P4HB was correlated with age ($P = 0.021$), Bormann type ($P = 0.029$), depth of tumor invasion ($P = 0.001$), lymph node metastasis ($P = 0.018$), postoperative adjuvant chemotherapy ($P = 0.008$), while GRP78 expression was only correlated with depth of tumor invasion ($P = 0.041$) and lymph node metastasis ($P = 0.043$) (Table 1). We also found P4HB expression was strongly correlated with GRP78 ($P < 0.001$). Spearman rank correlation analysis of P4HB and GRP78 H-scores proved this significant positive correlation ($R = 0.587$, $P < 0.001$) (sFigure 1A). By investigating the correlation coefficients of different clinicopathological characteristics, the correlation coefficients were significantly elevated in tumor size ≥ 5 cm ($P = 0.037$), TNM III/IV stage ($P = 0.017$) and positive vessel invasion ($P = 0.049$) subgroups, as shown in s (Table 2).

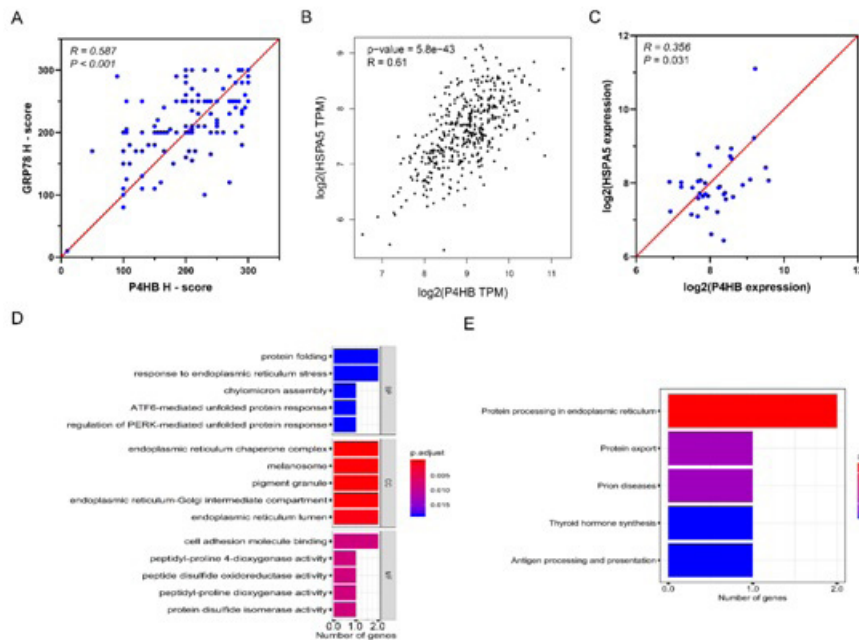
Table 1: Relationship between P4HB/GRP78 protein expression and clinicopathological characteristics in GC patients

Clinicopathological parameters	P4HB expression				GRP78 expression			
	Low	High	χ^2	P value	Low	High	χ^2	P value
	74	76			71	79		
Age(year)			5.369	0.021			2.404	0.121
<65	48	35			44	39		
≥ 65	26	41			27	40		
Gender			0.408	0.523			0.008	0.931
Male	49	54			49	54		
Female	25	22			22	25		
Bormann type			4.743	0.029			0.018	0.894
I / II	32	20			25	27		
III/IV	42	56			46	52		
Tumor size(cm)			0.455	0.5			0.318	0.573
<5	43	40			41	42		

≥5	31	36			30	37		
Lauren's classification			5.489	0.064			2.263	0.323
Intestinal	17	14			12	19		
Diffuse	40	31			38	33		
Mixed	17	31			21	27		
Differentiation			0.218	0.641			0.04	0.841
Well/Moderate	31	29			29	31		
Poor	43	47			42	48		
Histological type			2.599	0.107			3.071	0.08
Adenocarcinoma	66	73			63	76		
Mucinous/Signet-ring cell	8	3			8	3		
Depth of tumor invasion			11.786	0.001			4.192	0.041
T1/T2/T3	61	43			55	49		
T4	13	33			16	30		
Lymph node metastasis			5.561	0.018			4.092	0.043
Negative	32	19			30	21		
Positive	42	57			41	58		
TNM stage			3.209	0.073			0.914	0.339
I / II	41	31			37	35		
III / IV	33	45			34	44		
Vessel invasion			0.064	0.8			0.609	0.435
Negative	53	53			48	58		
Positive	21	23			23	21		
Perineural invasion			0.08	0.777			0.028	0.867
Negative	56	59			54	61		
Positive	18	17			17	18		
Postoperative adjuvant chemotherapy			7.055	0.008			0.334	0.563
No	17	33			22	28		
Yes	57	43			59	51		
GRP78 expression			34.562	<0.001				
Low	53	18						
High	21	58						

Table 2: Correlation between P4HB/HSPA5 with genes in UPR pathways from TCGA–STAD cohort

Pathway	Name in pathway	Typical encoded gene	P4HB		HSPA5	
			R	P value	R	P value
PERK pathway						
	PERK	EIF2AK3	0.48	<0.001	0.52	<0.001
	eIF1a	EIF2S1	0.41	<0.001	0.53	<0.001
	ATF4	ATF4	0.19	<0.001	0.22	<0.001
	GADD34	PPP1R15A	0.22	<0.001	0.3	<0.001
ATF6 pathway						
	NRF2	NFE2L2	0.27	<0.001	0.31	<0.001
	ATF6	ATF6	0.35	<0.001	0.52	<0.001
	S1P	MBTSP1	0.3	<0.001	0.41	<0.001
	S2P	MBTSP2	0.29	<0.001	0.41	<0.001
IRE1 pathway						
	WFS1	WFS1	0.25	<0.001	0.18	<0.001
	IRE1	ERN1	0.47	<0.001	0.29	<0.001
	TRAF2	TRAF2	0.41	<0.001	0.41	<0.001
	ASK1	MAP3K5	0.2	<0.001	0.31	<0.001
	MKK7	MAP2K7	0.22	<0.001	0.11	0.021
	JNK	MAPK8	0.31	<0.001	0.42	<0.001
	XBP	XBP1	0.48	<0.001	0.38	<0.001



sFigure 1: Correlation and bioinformatics analyses of P4HB and GRP78 (HSPA5) expressions in GC. A: The correlation of P4HB and GRP78 H-score; B: The correlation of P4HB and GRP78 in TCGA-STAD; C: The correlation of P4HB and GRP78 in CCLE; D: Gene Ontology (GO) analysis of P4HB and HSPA5. E: Kyoto Encyclopedia of Genes and Genomes (KEGG) analysis of P4HB and HSPA5. TCGA: the cancer genome atlas; STAD: stomach adenocarcinoma; CCLE: cancer cell line encyclopedia; BP: biological process; CC: cellular component; MF: molecular function.

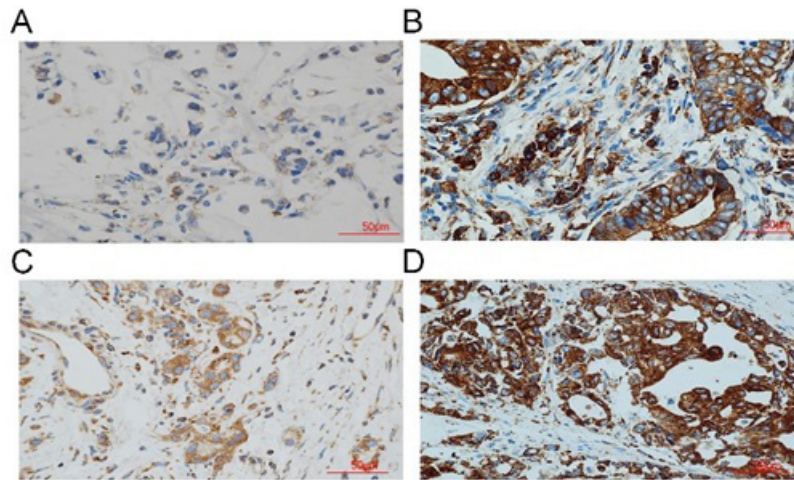
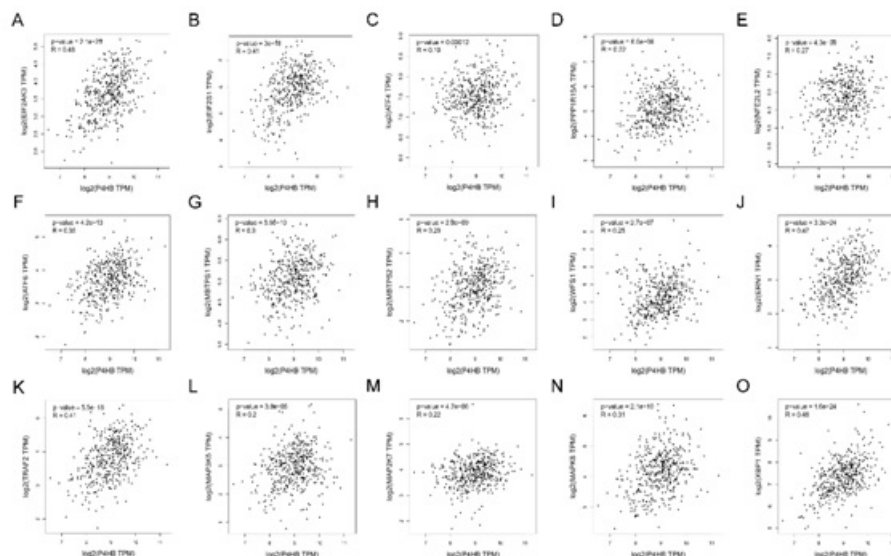


Figure 1: Representative immunohistochemical staining images of P4HB and GRP78 in gastric cancer (GC) tissues. A: Low expression of P4HB in the cytoplasm of a GC case. B: High expression of P4HB in the cytoplasm of a GC case. C: Low expression of GRP78 in the cytoplasm of a GC case. D: High expression of GRP78 in the cytoplasm of a GC case. Magnifications in all figures were 400 ×.

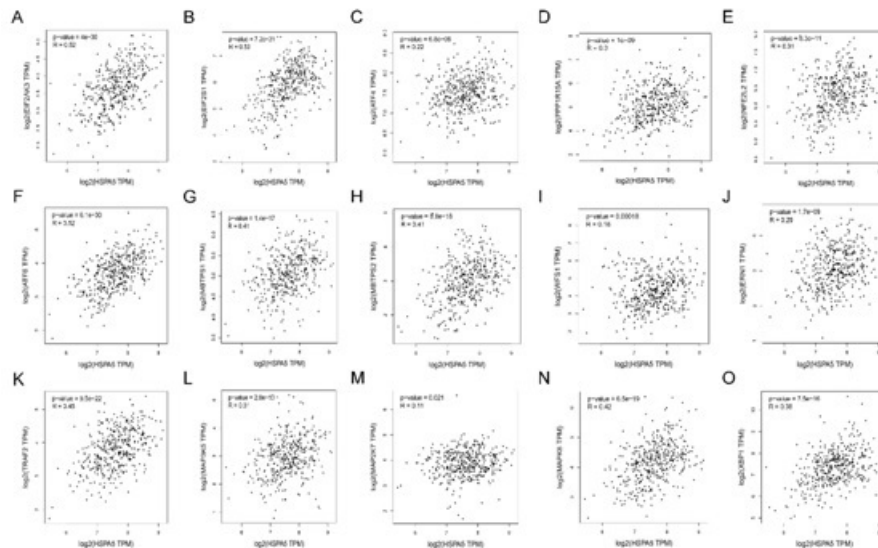
4.2. Bioinformatics analyses of P4HB and GRP78 expression in GC

We explored TCGA-STAD (stomach adenocarcinoma) data by GEPIA and analyzed of extracted 37 GC cell lines data from CCLE successively. It turned out P4HB mRNA was also positive correlated with GRP78 in both tissue and cell databases of GC ($R = 0.61$, $P < 0.001$, and $R = 0.356$, $P = 0.031$, respectively) (sFigure 1B and 1C), in accordance with the correlation of proteins. Furthermore, we performed GO and KEGG analysis of these two genes. The top 5 items of each GO term was shown in (sFigure 1D), only items involve with both two genes were taken into account. As a result, protein folding and response to ER stress were discovered in biological process (BP) term. ER chaperone complex, melanosome, pigment granule, ER-Golgi intermediate com-

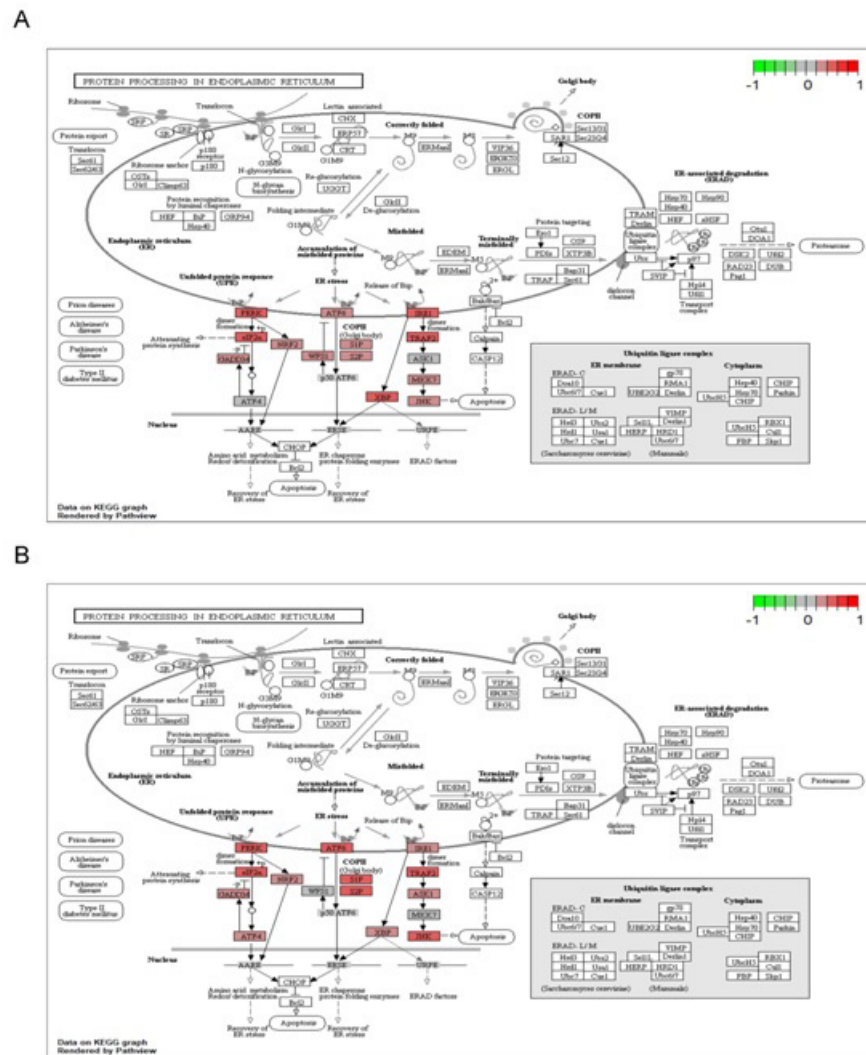
partment and ER lumen were discovered in cellular component (CC) term. Together with only cell adhesion molecule binding was discovered in molecular function (MF) term. KEGG pathway analysis showed both two genes were enriched in the pathway “protein processing in ER” (sFigure 1E). Due to the occurrence and development of GC may relate to ER stress and UPR, we made further efforts to search correlation of P4HB or HSPA5 with UPR genes, which from the “protein processing in ER” KEGG pathway map (hsa04141), through exploring TCGA-STAD cohort of GEPIA (sFigure 2-3). Except for both P4HB and HSPA5 positive correlated with typical UPR genes of STAD (Table 2), correlation coefficients of most upstream genes were higher than downstream genes, as shown in (sFigure 4).



sFigure 2: Correlation of P4HB and typical genes within UPR from TCGA-STAD. UPR: unfolded protein response; TCGA: the cancer genome atlas; STAD: stomach adenocarcinoma.



sFigure 3: The correlation of HSPA5 (GRP78) and typical genes within UPR from TCGA-STAD. UPR: unfolded protein response; TCGA: the cancer genome atlas; STAD: stomach adenocarcinoma.



sFigure 4: Correlation coefficients of P4HB and GRP78 (HSPA5) and typical genes within UPR from TCGA-STAD. A: Correlation coefficients of P4HB and typical genes within UPR from TCGA-STAD performed in KEGG pathway map. B: Correlation coefficients of HSPA5 and typical genes within UPR from TCGA-STAD performed in KEGG pathway map. UPR: unfolded protein response; TCGA: the cancer genome atlas; STAD: stomach adenocarcinoma.

4.3. Association of P4HB and GRP78 expression with OS in GC

Stratified by P4HB and GRP78 expression, we conducted Kaplan-Meier survival analysis and log-rank test to compare OS. The results revealed high expression of P4HB (Figure 2A) or GRP78 (Figure 2B) was related to an obvious shorter OS ($P < 0.001$ and $P = 0.012$, respectively). Further analysis showed when both low expressed P4HB and GRP78, the prognosis was the best, and the worst prognosis was correlated with high expression of both P4HB and GRP78, while high expressed only one protein, the prognosis was in between (Figure 2C, $P = 0.002$). As well as OS of the both or one high expression group was sharp shorter than both low expression group (Figure 2D, $P = 0.002$).

Since P4HB and GRP78 were both reported to be associated

with chemotherapy, we further explored the prognosis of fluorouracil-based postoperative adjuvant chemotherapy together with co-expression of P4HB and GRP78. We observed the prognosis of group with postoperative adjuvant chemotherapy was better than another group (Figure 2E, $P = 0.011$), high level of P4HB and/or GRP78 exhibited a significant worse OS in the former group (Figure 2F, $P = 0.007$), but no difference in the latter group (Figure 2G, $P = 0.231$). When the group with postoperative adjuvant chemotherapy stratified by TNM stage, it exhibited no prognostic significance in TNM I / II stage (Figure 2H, $P = 0.859$), although a significant worse OS if high co-expression in TNM III/IV stage subgroup (Figure 2I, $P = 0.004$). This indicated GC patients in TNM III/IV stage might benefit less from postoperative adjuvant chemotherapy once P4HB and/or GRP78 high expressed.

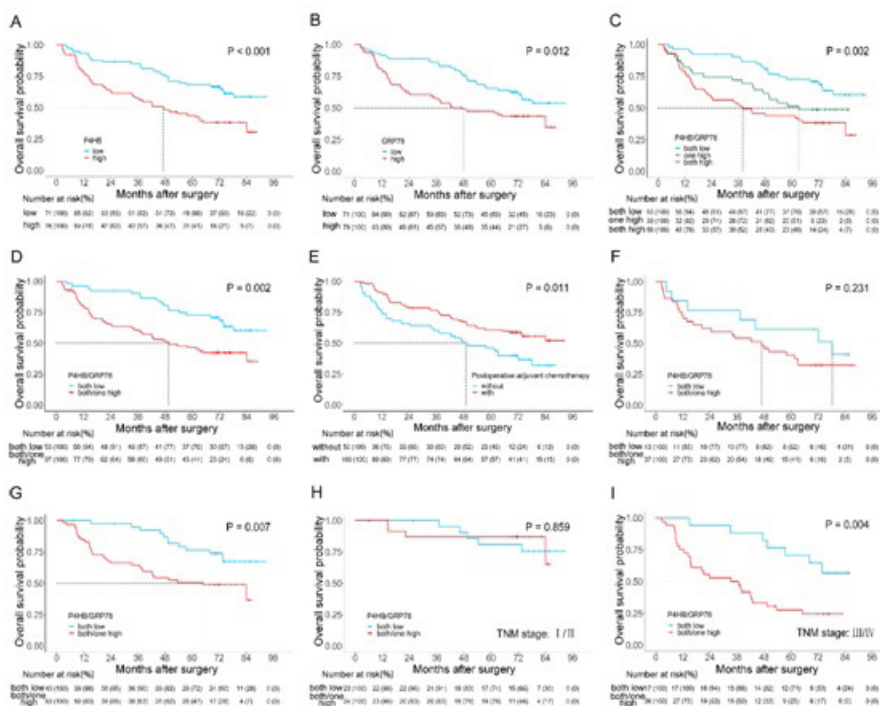


Figure 2: Kaplan-Meier analyses of OS in GC patients. A: Kaplan-Meier analysis of OS according to single P4HB expression. B: Kaplan-Meier analysis of OS according to single GRP78 expression. C and D: Kaplan-Meier analysis of OS according to combined P4HB and GRP78 expression. E: Kaplan-Meier analysis of OS according to postoperative adjuvant chemotherapy. F: Kaplan-Meier analysis of OS in patients without postoperative adjuvant chemotherapy according to co-expression of P4HB and GRP78. G: Kaplan-Meier analysis of OS in patients with postoperative adjuvant chemotherapy according to co-expression of P4HB and GRP78. H: OS curves of stage I / II patients with postoperative adjuvant chemotherapy stratified by co-expression of P4HB and GRP78. I: OS curves of stage III/IV patients with postoperative adjuvant chemotherapy stratified by co-expression of P4HB and GRP78.

4.4. Construction of a nomogram based on stepwise Cox regression analysis

Univariate analyses were performed for clinicopathological characteristics to estimate postoperative survival. As shown in (Table 3), we observed OS was correlated with Bormann type ($P = 0.004$), tumor size ($P = 0.028$), differentiation ($P = 0.004$), depth of tumor invasion ($P < 0.001$), lymph node metastasis ($P < 0.001$), TNM stage ($P < 0.001$), postoperative adjuvant chemotherapy ($P = 0.012$), P4HB expression ($P = 0.001$), GRP78 expression ($P =$

0.013), P4HB and GRP78 co-expression ($P = 0.002$). These above variables were subsequent recruited to forward stepwise COX analysis, it turned out differentiation ($P = 0.020$, HR = 1.846, 95% CI: 1.099-3.101), TNM stage ($P < 0.001$, HR = 3.124, 95% CI: 1.870-5.217), postoperative adjuvant chemotherapy ($P = 0.005$, HR = 0.507, 95% CI: 0.317-0.810), P4HB and GRP78 co-expression ($P = 0.002$, HR = 2.304, 95% CI: 1.355-3.915) were independent prognostic factors (Table 3). The four independent prognostic factors were further recruited to construct a nomogram for predict-

ing OS probability of GC patients (Figure 3A), whose Harrell's C-index was 0.733 (95% CI: 0.680-0.786). And calibration plots for the nomogram indicated the model was well calibrated, since they were close to the 45-degree line (the perfect calibration model) at 3-year and 5-year (Figure 3B and 3C).

Table 3: Univariate and multivariate analyses of prognostic characteristics for overall survival in patients with gastric cancer

Variables	Univariate analysis			Multivariate analysis		
	HR	(95%CI)	P value	HR	(95%CI)	P value
Age(year)						
≥65 vs. <65	1.246	0.791-1.963	0.343			
Gender						
Female vs. Male	1.081	0.665-1.756	0.754			
Bormann type						
III/IV vs. I / II	2.142	1.271-3.609	0.004			
Tumor size(cm)						
≥5 vs. <5	1.662	1.056-2.616	0.028			
Lauren's classification			0.214			
Intestinal	1	Reference				
Diffuse	1.818	0.932-3.545	0.079			
Mixed	1.613	0.790-3.293	0.19			
Differentiation						
Poor vs. Well/Moderate	2.111	1.274-3.497	0.004	1.846	1.099-3.101	0.02
Histological type						
Mucinous/Signet-ring cell	0.592	0.216-1.622	0.308			
vs. Adenocarcinoma						
Depth of tumor invasion						
T4 vs. T1/T2/T3	2.536	1.601-4.019	<0.001			
Lymph node metastasis						
Positive vs. Negative	3.824	2.060-7.101	<0.001			
TNM stage						
III/IV vs. I / II	3.2	1.942-5.275	<0.001	3.124	1.870-5.217	<0.001
Vessel invasion						
Positive vs. Negative	1.385	0.861-2.229	0.18			

Perineural invasion							
Positive vs. Negative	1.279	0.766-2.135	0.346				
Postoperative adjuvant chemotherapy							
Yes vs. No	0.556	0.351-0.879	0.012	0.507	0.317-0.810	0.005	
P4HB expression							
High vs. Low	2.266	1.414-3.630	0.001				
GRP78 expression							
High vs. Low	1.799	1.130-2.862	0.013				
P4HB and GRP78 co-expression							
Both/one high vs. Both low	2.26	1.338-3.817	0.002	2.304	1.355-3.915	0.002	

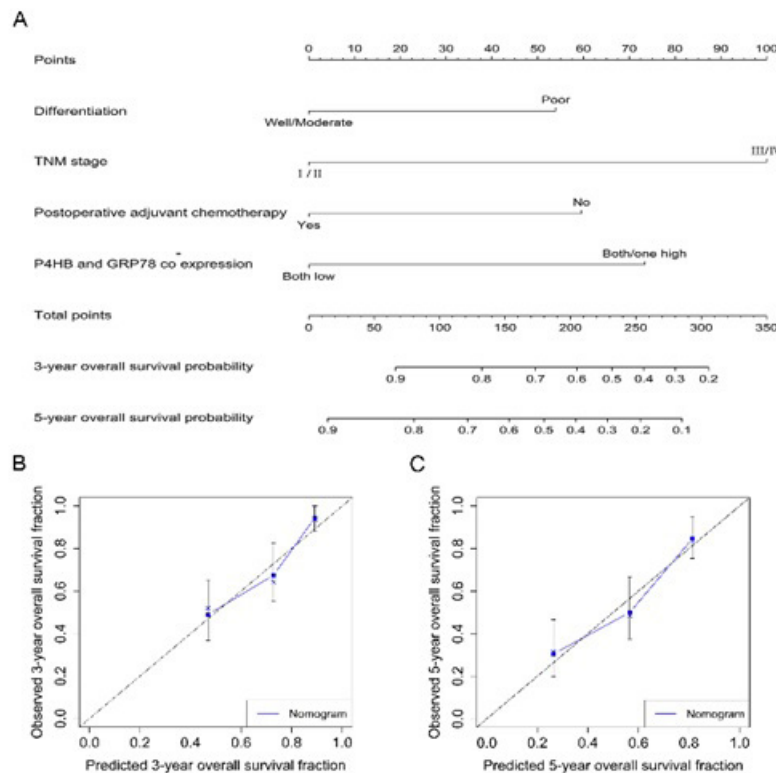


Figure 3: Nomogram and calibration plots for OS prediction in GC patients. A: Nomogram for predicting 3-year and 5-year OS probabilities; B: Calibration plot for predicting 3-year OS; C: Calibration plot for predicting 5-year OS.

4.5. Evaluate the nomogram and its clinical value with TNM stage

To evaluate discrimination ability and clinical usefulness of the nomogram, we compared it with widely clinical used TNM stage. From (Figure 4A and 4B), we found areas under receiver operating characteristic curve (AUCs) of the 3-year and 5-year OS probability were 0.790 and 0.760, respectively, much larger than TNM stage

(0.684 and 0.671, respectively), proved discrimination ability of the nomogram was better. Since DCA has advantages over AUC for estimating alternative prognostic strategies, we performed the 3-year and 5-year DCA curves individually of the nomogram and TNM stage. As shown in (Figure 4C and 4D), compared to TNM stage, the nomogram offered a higher net benefit in 3-year and 5-year, respectively, even at an extremely small threshold probability.

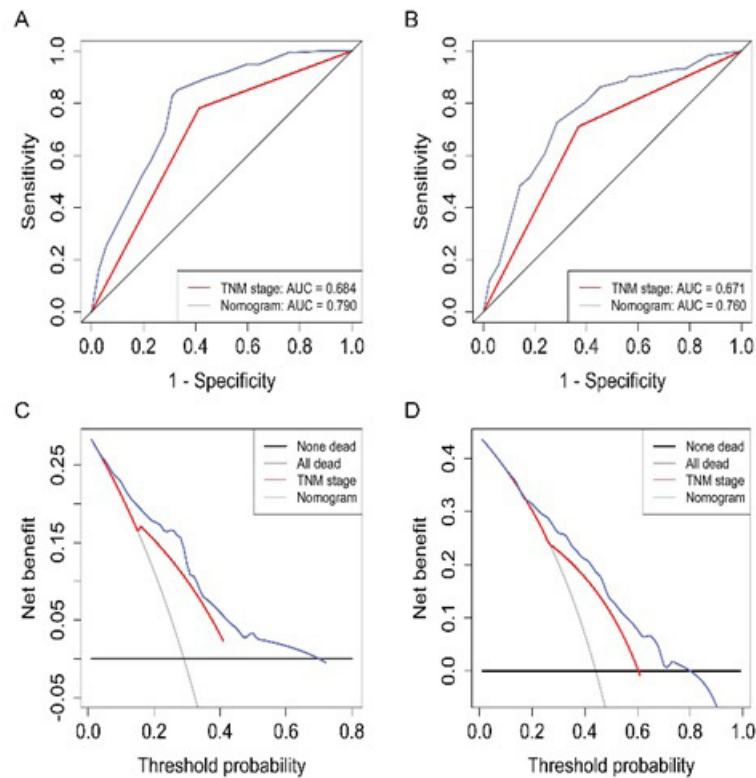


Figure 4: ROC and DCA curves of nomogram and TNM stage for OS prediction in GC patients. A: ROC curves for predicting 3-year OS; B: ROC curves for predicting 5-year OS; C: DCA curves for predicting 3-year OS; D: DCA curves for predicting 5-year OS.

5. Discussion

ER not only is high in calcium-dependent molecular chaperones such as GRP78 for stabilizing protein-folding intermediates, also offers an oxidative environment for the formation of disulphide bonds with the aid of PDI and for the proper folding of proteins [23, 24]. Under non-stressed conditions, GRP78 combines with three UPR sensors (PERK, ATF6 and IRE1) to keep them inactive. Once ER stress occurs, GRP78 preferentially binds to the unfolded proteins, dissociates from the sensors, resulting in activation of the UPR transducers [6, 25]. The outcome involves in protein folding and transporting, as well as increasing unfolded protein clearance through pathways such as ER-associated degradation (ERAD) and autophagy. And cells will meet apoptosis upon unresolved stress [8].

PDI family, part of the thioredoxin superfamily, mainly acts as catalysts for the formatting and rearranging S-S bonds, also can function as chaperones within ERAD [26], contributes a lot to maintain and regulate proteostasis. P4HB, also known as PDIA1 (usually referred as PDI), as the archetype PDI protein, the chaperone activity of whom is independent of catalytic activity, is vital for many client proteins [27]. There is sufficient evidence supporting that PDIA1 high expressed in a wide variety of cancers tissues [9-11, 24] and cancer cells [28], the upregulated PDIA1 is close correlated with cancer metastasis and invasiveness [27]. GRP78 is encoded by HSPA5, as the most abundant protein of heat shock protein-70 family, mainly exists in ER lumen, prevents

the transport of misfolded proteins or protein subunits, expect for correcting the folding and assembly [29, 30]. GRP78 works as a molecular chaperone in cells, whose high expression is crucial for proliferation, invasion, metastasis of many cancers, proves to be correlated with tumor resistance, recurrence, and a low OS [17, 18, 31-33]. With the help of GRP78, tumor cells can organize the stimulation of processes including combat reactive oxygen species, macroautophagy, and enable pro-survival signaling pathways [29]. Thus, GRP78 will be a useful prognostic biomarker and a promising target for cancer.

P4HB and GRP78 are both ER chaperone proteins involved in UPR, and represent for poor prognosis of various cancers from the above mentioned. However, rare research pays attention to the correlation of them, especially in cancer. An early study shows that BiP and PDI perform synergistically in vitro in the oxidative folding of antibodies, BiP bind to the unfolded polypeptide chains to keep them in a conformation where cysteine residues are accessible for PDI [34]. Different from P4HB negative correlated with GRP78 in hepatocellular cancer in vitro [19], we confirmed that P4HB and GRP78 showed a positive correlation in protein (from our cohort) and mRNA (from the databases) levels. With the development of disease, the relationship might be closer since correlation coefficients were significantly elevated in tumor size ≥ 5 cm, TNM III/IV stage and positive vessel invasion subgroups. Besides, single or combined high expression of P4HB and GRP78 represented for poor prognosis in GC. While the specific mecha-

nisms need further exploration.

A lot of studies have shown in a wide range of primary tumors, there exists a sustained and high-level activation of all three branches within UPR [35]. From bioinformatics analyses, we also found P4HB and GRP78 might participate in UPR, since they positive correlated with all typical UPR genes, together with correlation coefficients of most upstream genes were higher than downstream genes. UPR may act as a key driver in resistance to chemotherapy [36, 37]. A new encouraging research finds that activation of the PERK branch with UPR is required for colon cancer cells surviving from treatment of 5-fluorouracil, the usage of PERK inhibitor synergizes with 5-FU could suppress the growth of colon cancer cells in vivo [38]. It may explain in fluorouracil-based postoperative adjuvant chemotherapy subgroup, GC patients with a high co-expression of P4HB and GRP78 had a shorter OS of our cohort. When stratified by TNM stage, only patients in TNM III/IV stage had a significant shorter OS. One reason might be that in early stage GC, the positive effects from chemotherapy could cancel out the negative effects from UPR, while in advanced GC, the negative effects probably could have exceeded the positive effects. Our nomogram integrated co-expression of P4HB and GRP78 with other prognostic variables, was a simple visualized tool for predicting OS after surgery of GC patients. Comparing to TNM stage, the discrimination ability and clinical usefulness of the nomogram was much better through AUCs and DCA curves of 3-year and 5-year, may be of a great value for clinic. There still remain several limitations in our study. Firstly, this is a retrospective study of small sample group of GC patients, exists the statistical limitations. Secondly, further researches are required to confirm the correlation and regulation mechanisms of P4HB and GRP78 expression of GC in vitro and in vivo. Finally, it needs an independent external cohort to verify our research findings. In conclusion, we reveal that P4HB expression positive correlate with GRP78 in GC, may involve in UPR, and the relationship will be closer in advanced GC. High co-expression of P4HB and GRP78 may predict a shorter OS with fluorouracil-based postoperative adjuvant chemotherapy in the advanced stage. On the other hand, the co-expression of them can independently predict unfavorable OS for GC patients. As well as the prognostic nomogram based on stepwise Cox regression model may be better than TNM stage in discrimination ability and clinical usefulness.

6. Acknowledgement

We thank all the contributors for this work. This work was supported by Natural Science Foundation of Jiangsu Province(BK20191208); Basic Science Research Project of Nantong(-JC2018031) ;the Youth Science and Research Foundation of Nantong Health Commission (QA2019025).

7. Authors' contributions

Zhang CF and Zhao WJ performed the majority of experiments

and wrote the manuscript; Yang L and Chen XD designed and supervised the study; Zhang XS assisted in conducting the IHC assays; Zhang XL,Xu WW and Song L collected and analyzed the data.

8. Availability of Data and Materials

All data and material are available from the corresponding author.

9. Ethics Approval and Consent to Participate

This research was reviewed and approved by the Ethics Committee of Affiliated Tumor Hospital of Nantong University.

10. Consent for Publication

The publication of this manuscript has been approved by all authors.

11. Competing Interests

The authors declare that they have no competing interests.

References

1. Bray F, Ferlay J, Soerjomataram I, Siegel RL, Torre LA, Jemal A, et al. Global cancer statistics 2018: GLOBOCAN estimates of incidence and mortality worldwide for 36 cancers in 185 countries. *CA Cancer J Clin.* 2018; 68(6): 394-424.
2. Cutsem EV, Sagaert X, Topal B, Haustermans K, Prenen H. Gastric cancer. *The Lancet.* 2016; 388(10060): 2654-2664.
3. Allemani C, Matsuda T, Di Carlo V, Harewood R, Matz M, Niksis M, et al. Global surveillance of trends in cancer survival 2000–14 (CONCORD-3): analysis of individual records for 37 513 025 patients diagnosed with one of 18 cancers from 322 population-based registries in 71 countries. *The Lancet.* 2018; 391(10125): 1023-1075.
4. Setia N, Agoston AT, Han HS, Mullen JT, Duda DG, Clark JW, et al. A protein and mRNA expression-based classification of gastric cancer. *Mod Pathol.* 2016; 29(7): 772-784.
5. Jiang Y, Zhang Q, Hu Y, Li T, Yu J, Zhao L, et al: ImmunoScore Signature: A Prognostic and Predictive Tool in Gastric Cancer. *Ann Surg.* 2018; 267(3): 504-513.
6. Tameire F, Verginadis, II, Koumenis C. Cell intrinsic and extrinsic activators of the unfolded protein response in cancer: Mechanisms and targets for therapy. *Semin Cancer Biol.* 2015; 33: 3-15.
7. Kranz P, Neumann F, Wolf A, Classen F, Pomsch M, Ocklenburg T, et al. PDI is an essential redox-sensitive activator of PERK during the unfolded protein response (UPR). *Cell Death Dis.* 2017; 8(8): e2986.
8. Wang M, Kaufman RJ. The impact of the endoplasmic reticulum protein-folding environment on cancer development. *Nat Rev Cancer.* 2014; 14(9): 581-597.
9. Zou H, Wen C, Peng Z, Shao Y, Hu L, Li S, et al. P4HB and PDIA3 are associated with tumor progression and therapeutic outcome of diffuse gliomas. *Oncol Rep.* 2018; 39(2): 501-510.
10. Wang SM, Lin LZ, Zhou DH, Zhou JX, Xiong SQ. Expression of prolyl 4-hydroxylase beta-polypeptide in non-small cell lung cancer treated with Chinese medicines. *Chin J Integr Med.* 2015; 21(9): 689-696.

11. Zhou Y, Yang J, Zhang Q, Xu Q, Lu L, Wang J, et al. P4HB knock-down induces human HT29 colon cancer cell apoptosis through the generation of reactive oxygen species and inactivation of STAT3 signaling. *Mol Med Rep.* 2019; 19(1): 231-237.
12. Xu S, Sankar S, Neamati N. Protein disulfide isomerase: a promising target for cancer therapy. *Drug Discov Today.* 2014; 19(3): 222-240.
13. Liu Z, Wang Y, Wang Y, Dong W, Xia X, Song E, et al. Effect of Sub-cellular Translocation of Protein Disulfide Isomerase on Tetrachloro-benzoquinone-Induced Signaling Shift from Endoplasmic Reticulum Stress to Apoptosis. *Chem Res Toxicol.* 2017; 30(10): 1804-1814.
14. Kullmann M, Kalayda GV, Hellwig M, Kotz S, Hilger RA, Metzger S, et al. Assessing the contribution of the two protein disulfide isomerases PDIA1 and PDIA3 to cisplatin resistance. *J Inorg Biochem.* 2015; 153: 247-252.
15. Zhang J, Wu Y, Lin YH, Guo S, Ning PF, Zheng ZC, et al. Prognostic value of hypoxia-inducible factor-1 alpha and prolyl 4-hydroxylase beta polypeptide overexpression in gastric cancer. *World J Gastroenterol.* 2018; 24(22): 2381-2391.
16. Kwon D, Koh J, Kim S, Go H, Min HS, Kim YA, et al. Overexpression of endoplasmic reticulum stress-related proteins, XBP1s and GRP78, predicts poor prognosis in pulmonary adenocarcinoma. *Lung Cancer.* 2018; 122: 131-137.
17. Nagelkerke A, Bussink J, Sweep FC, Span PN. The unfolded protein response as a target for cancer therapy. *Biochim Biophys Acta.* 2014; 1846(2): 277-284.
18. Gifford JB, Hill R. GRP78 Influences Chemoresistance and Prognosis in Cancer. *Curr Drug Targets.* 2018; 19(6): 701-708.
19. Xia W, Zhuang J, Wang G, Ni J, Wang J, Ye Y, et al. P4HB promotes HCC tumorigenesis through downregulation of GRP78 and subsequent upregulation of epithelial-to-mesenchymal transition. *Oncotarget.* 2017; 8(5): 8512-8521.
20. Li L, Cui Y, Ji JF, Jiang WG. Clinical Correlation Between WISP2 and beta-Catenin in Gastric Cancer. *Anticancer Res.* 2017; 37(8): 4469-4473.
21. Tang Z, Li C, Kang B, Gao G, Li C, Zhang Z, et al. GEPIA: a web server for cancer and normal gene expression profiling and interactive analyses. *Nucleic Acids Res.* 2017; 45(W1): W98-W102.
22. Barretina J, Caponigro G, Stransky N, Venkatesan K, Margolin AA, Kim S, et al. The Cancer Cell Line Encyclopedia enables predictive modelling of anticancer drug sensitivity. *Nature.* 2012; 483(7391): 603-607.
23. Kim I, Xu W, Reed JC. Cell death and endoplasmic reticulum stress: disease relevance and therapeutic opportunities. *Nat Rev Drug Discov.* 2008; 7(12): 1013-1030.
24. Maattanen P, Gehring K, Bergeron JJ, Thomas DY. Protein quality control in the ER: the recognition of misfolded proteins. *Semin Cell Dev Biol.* 2010; 21(5): 500-511.
25. Lai E, Teodoro T, Volchuk A. Endoplasmic Reticulum Stress: Signaling the Unfolded Protein Response. *Physiology.* 2007; 22: 193-201.
26. Hatahet F, Ruddock LW. Substrate recognition by the protein disulfide isomerases. *FEBS Journal* 2007; 274(20): 5223-5234.
27. Lee E, Lee DH. Emerging roles of protein disulfide isomerase in cancer. *BMB Rep.* 2017; 50(8): 401-410.
28. Shin BK, Wang H, Yim AM, Le Naour F, Brichory F, Jang JH, et al. Global profiling of the cell surface proteome of cancer cells uncovers an abundance of proteins with chaperone function. *J Biol Chem.* 2003; 278(9): 7607-7616.
29. Casas C. GRP78 at the Centre of the Stage in Cancer and Neuroprotection. *Frontiers in Neuroscience.* 2017; 11: 177.
30. Ibrahim IM, Abdelmalek DH, Elfiky AA. GRP78: A cell's response to stress. *Life Sciences.* 2019; 226: 156-163.
31. Guan M, Chen X, Ma Y, Tang L, Guan L, Ren X, et al. MDA-9 and GRP78 as potential diagnostic biomarkers for early detection of melanoma metastasis. *Tumor Biology.* 2014; 36(4): 2973-2982.
32. Mhaidat NM, Alzoubi KH, Almomani N, Khabour OF. Expression of glucose regulated protein 78 (GRP78) determines colorectal cancer response to chemotherapy. *Cancer Biomark.* 2015; 15(2): 197-203.
33. Dai YJ, Qiu YB, Jiang R, Xu M, Liao LY, Chen GG, et al. Concomitant high expression of ERalpha36, GRP78 and GRP94 is associated with aggressive papillary thyroid cancer behavior. *Cell Oncol (Dordr).* 2018; 41(3): 269-282.
34. Mayer M, Kies U, Kammermeier R, Buchner J. BiP and PDI cooperate in the oxidative folding of antibodies in vitro. *J Biol Chem.* 2000; 275(38): 29421-29425.
35. Oakes SA, Papa FR. The role of endoplasmic reticulum stress in human pathology. *Annu Rev Pathol.* 2015; 10: 173-194.
36. Wang Y, Wang K, Jin Y, Sheng X. Endoplasmic reticulum proteostasis control and gastric cancer. *Cancer Lett.* 2019; 449: 263-271.
37. Kim C, Kim B. Anti-Cancer Natural Products and Their Bioactive Compounds Inducing ER Stress-Mediated Apoptosis: A Review. *Nutrients.* 2018; 10(8): 1021.
38. Shi Z, Yu X, Yuan M, Lv W, Feng T, Bai R, et al. Activation of the PERK-ATF4 pathway promotes chemo-resistance in colon cancer cells. *Sci Rep.* 2019; 9(1): 3210.